Biochimica et Biophysica Acta, 735 (1983) 397–406
Elsevier

BBA 71888

LIGHT-SCATTERING PROPERTIES OF OSMOTICALLY ACTIVE LIPOSOMES

WATARU YOSHIKAWA, HIDEO AKUTSU and YOSHIMASA KYOGOKU
Institute for Protein Research, Osaka University, Suita, Osaka 565 (Japan)

(Received July 15th, 1983)

Key words: Liposome; Light scattering; Osmotic behavior; Size determination

Scattering efficiency and turbidity of multilamellar liposomes were calculated on the basis of the Mie theory using both multishelled and homogeneous sphere models. A multishelled sphere model which is composed of alternate lipid and water layers can be well approximated by a homogeneous sphere model with the average refractive index of the two components. It is also shown that turbidity (τ) of liposomes is reciprocally proportional to the two-thirds power of the total volume (V) upon swelling and shrinking of liposomes through a change in water content. The contribution of the size distribution was also taken into account in the estimation. Our calculation revised the empirical relationship ($V \propto 1/\tau$) proposed by Bangham, but gave theoretical support to his idea that the turbidimetric method is useful for measuring relative sizes of osmotically active liposomes. The relationship was checked for the real liposome systems of egg-yolk phosphatidylcholine and phosphatidic acid. The deviation from the theoretical curve under hypotonic conditions was explained by partial leakage of the contents from the inside through measuring radioactivity of [^{14}C]glucose.

Introduction

Multilamellar liposomes of phospholipids including a small amount of charged lipids were shown to be osmotically active and the osmotic behaviors were investigated using turbidimetry by Bangham et al. [1] and Rendi [2]. They deduced an empirical relationship between the volume and the turbidity of liposomes. Namely, the total volume of liposomes is reciprocally proportional to the turbidity at 450 nm. The turbidimetric (optical) method is based on this relationship. Turbidity is easily measured and the sensitivity of the method is high enough to follow a rapid volume change of liposomes without any perturbation of the system. Hence, it has also been used to investigate the permeability of water or solute through the liposomal membrane [1,3–6]. In spite of the promising possibilities of the method, it is not yet well used, since the theoretical background of the empirical relationship has not been elucidated.

Koch investigated turbidity of intact mitochondrial and bacterial suspensions given that the radius involved is very large and the refractive index is very small [7]. He concluded from the calculation based on the Jobst approximation [8] that the turbidity of the suspension is reciprocally proportional to the two-thirds power of the particle volume. It was further indicated that a change of turbidity upon swelling or shrinking of mitochondria should satisfy the relationship.

The multilamellar liposome prepared by a hand-shaken method assumes an onion-like structure with alternate phospholipid and water layers [9,10]. To explain the osmotically induced change of turbidity, light-scattering of multishelled spheres as a model of multilamellar liposomes was examined in this work. Calculation was carried out according to the Mie theory [11], which is applicable to multishelled spheres of arbitrary size [12].

The results suggest that under certain conditions, the turbidity of a multishelled sphere suspension is approximately the same as that of homogeneous spheres of average refractive index. It is also shown that turbidity is reciprocally proportional to the two-thirds power of the volume of the sphere and the size distribution of a multishelled sphere does not affect this relationship. This was confirmed by an actual liposomal system of egg-yolk phosphatidylcholine and phosphatidic acid. Our results provide a theoretical background to the turbidimetric method in the investigation of the properties of osmotically active liposomes.

Theory

The turbidity of a suspension of particles, τ, is a measure of the reduction of the intensity of the beam due to scattering during the transmission and is defined by

$$\tau = 2.303A = (1/d)\cdot\ln(I_0/I) \tag{1}$$

where A is absorbance, d is the length of the light-path of the suspension and I_0 and I are the intensities of the incident and transmitted beams, respectively. For a dilute suspension of particles, the turbidity is given by

$$\tau = \nu\cdot\pi R^2\cdot K_t(m,\alpha) = \nu\cdot\frac{\lambda^2}{4\pi n_w^2}\cdot\alpha^2 K_t(m,\alpha) \tag{2}$$

where ν is the number concentration of the particles in the suspension, and R is the radius of the particle. K_t is the scattering efficiency defined as the ratio of scattering cross-section to geometric cross-section, and is a function of the parameter radius, $\alpha(=2\pi n_w R/\lambda$; n_w, refractive index of water at the wavelength λ of the beam), and the relative refractive index, $m(=n/n_w$; n, refractive index of the particle at λ) [12]. From Eqn. 2, the specific turbidity is given by

$$\frac{\tau}{c} = \frac{3\pi n_w}{2\rho\lambda}\cdot\frac{K_t}{\alpha} \tag{3}$$

where c is the concentration (mass per unit volume) of the particles and ρ is the density of the particle. The exact value of K_t can be evaluated according to the Mie theory of light-scattering of spherical particles, and is given by the following equation:

$$K_t = \frac{2}{\alpha^2}\cdot\sum_{n=1}^{\infty}(2n+1)\cdot\left\{|A_n|^2+|B_n|^2\right\} \tag{4}$$

$$A_n = \frac{\psi_n'(m\alpha)\psi_n(\alpha)-m\psi_n(m\alpha)\psi_n'(\alpha)}{\psi_n'(m\alpha)\zeta_n(\alpha)-m\psi_n(m\alpha)\zeta_n'(\alpha)} \tag{5a}$$

$$B_n = \frac{m\psi_n'(m\alpha)\psi_n(\alpha)-\psi_n(m\alpha)\psi_n'(\alpha)}{m\psi_n'(m\alpha)\zeta_n(\alpha)-\psi_n(m\alpha)\zeta_n'(\alpha)} \tag{5b}$$

where

$$\psi_n(x) = \sqrt{\pi x/2}\cdot J_{n+1/2}(x),\quad \psi_n'(x) = \mathrm{d}\psi_n(x)/\mathrm{d}x$$

$$\chi_n(x) = -(-1)^{n+1}\cdot\sqrt{\pi x/2}\cdot J_{-n-1/2}(x),$$

$$\chi_n'(x) = \mathrm{d}\chi_n(x)/\mathrm{d}x$$

$$\zeta_n(x) = \psi_n(x)+i\cdot\chi_n(x),\quad \zeta_n'(x) = \psi_n'(x)+i\cdot\chi_n'(x) \tag{6}$$

$J_{n+1/2}(x)$ is a half-integral-ordered Bessel function. Kerker extended this theory to multishelled spheres [12]. For a multishelled sphere composed of alternate water and lipid layers as shown in Fig. 1, A_n is expressed by the following equation.

$$A_n = \begin{vmatrix}
\psi_n'(\alpha_1) & \psi_n'(m\alpha_1) & \chi_n'(m\alpha_1) & 0 & 0 & \cdots & 0 & 0 & 0 \\
\psi_n(\alpha_1) & m\psi_n(m\alpha_1) & m\chi_n(m\alpha_1) & 0 & 0 & \cdots & 0 & 0 & 0 \\
0 & \psi_n'(m\alpha_2) & \chi_n'(m\alpha_2) & \psi_n'(\alpha_2) & \chi_n'(\alpha_2) & \cdots & 0 & 0 & 0 \\
0 & m\psi_n(m\alpha_2) & m\chi_n(m\alpha_2) & \psi_n(\alpha_2) & \chi_n(\alpha_2) & \cdots & 0 & 0 & 0 \\
0 & 0 & 0 & \psi_n'(\alpha_3) & \chi_n'(\alpha_3) & \cdots & 0 & 0 & 0 \\
0 & 0 & 0 & \psi_n(\alpha_3) & \chi_n(\alpha_3) & \cdots & 0 & 0 & 0 \\
0 & 0 & 0 & 0 & 0 & \cdots & 0 & 0 & 0 \\
0 & 0 & 0 & 0 & 0 & \cdots & \psi_n'(m\alpha_l) & \chi_n'(m\alpha_l) & \psi_n'(\alpha_l) \\
0 & 0 & 0 & 0 & 0 & \cdots & m\psi_n(m\alpha_l) & m\chi_n(m\alpha_l) & \psi_n(\alpha_l) \\
\multicolumn{9}{c}{\text{same as above except that } \psi_n'(\alpha_1) \text{ and } \psi_n(\alpha_1) \text{ are replaced by } \zeta_n'(\alpha_1) \text{ and } \zeta_n(\alpha_1)}
\end{vmatrix} \tag{7}$$

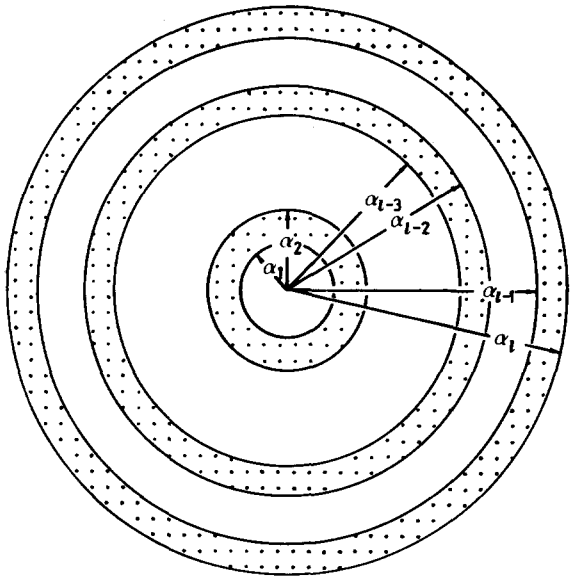

Fig. 1. Geometry of a multishelled sphere. The thickness of each lipid and each water shell is assumed to be the same. α_k is a parameter radius which is expressed as $\alpha_k = 2\pi n_w R_k/\lambda$, using the real radius R_k.

The equation for B_n can be obtained by raising 'm' terms from the even-numbered rows of the determinants to the odd-numbered rows immediately above; for example:

$$\psi_n'(m\alpha) \to m\psi'(m\alpha) \text{ and } m\psi_n(m\alpha) \to \psi_n(m\alpha)$$

In the actual multilamellar liposomes, there is a wide distribution in particle size. The specific turbidity in such a case is given by:

$$\frac{\tau}{c} = \frac{3\pi n_w}{2\rho\lambda^2} \cdot \int_0^\infty K_t(\alpha) \cdot \alpha^{-1} \cdot f(\alpha) \mathrm{d}\alpha \tag{8}$$

using the mass fraction $f(\alpha)$. A log-normal distribution with two parameters was assumed in this work, since it seems more appropriate than a symmetrical size distribution in view of the size distribution of liposomes observed by electron microscopy [25]. It leads to

$$f(\alpha)\mathrm{d}\alpha = \frac{1}{\sqrt{2\pi} \cdot \ln\sigma} \exp\left\{-\frac{1}{2}\left(\frac{\ln\alpha - \ln\alpha_{50}}{\ln\sigma}\right)^2\right\} \frac{\mathrm{d}\alpha}{\alpha} \tag{9}$$

where α_{50} is the geometric mean parameter radius and σ is the geometric standard deviation [13].

Materials and Methods

Calculation

Calculations were carried out on an ACOS-900 NEAC computer system in double-precision arithmetic. Bessel functions were calculated using the recurrence formula, namely

$$J_{P+1}(x) = \frac{2P}{x} \cdot J_P(x) - J_{P-1}(x) \tag{10}$$

$$J_{1/2}(x) = \sqrt{2/\pi x} \cdot \sin(x) \tag{11a}$$

$$J_{-1/2}(x) = \sqrt{2/\pi x} \cdot \cos(x) \tag{11b}$$

where P is an integer or half-integer. Derivatives were obtained according to the relationship

$$\frac{\mathrm{d}J_P}{\mathrm{d}x} = \tfrac{1}{2}(J_{P-1}(x) - J_{P+1}(x)) \tag{12}$$

Preparation of multilamellar liposomes

Egg-yolk phosphatidylcholine was purchased from Merck and purified by alumina column chromatography. Phosphatidic acid was obtained by enzymatic hydrolysis of egg-yolk phosphatidylcholine with phospholipase D extracted from Savoy cabbage [14]. All other reagents are commercial and of analytical grade. Stock dispersions for turbidimetric measurements were prepared as follows. An aliquot of a stock solution of lipids (phosphatidylcholine : phosphatidic acid = 96 : 4 w/w) in chloroform was put into a round-bottomed flask. The solvent was removed by a rotary evaporator to dryness and further under high vacuum for overnight. The lipid on the surface of the flask was suspended in an aqueous solution comprising 100 mM glucose/2 mM EDTA/10 mM Tris at pH 7.5 by a vortex mixer.

Optical measurement

0.2 ml of stock dispersion was mixed with 3.0 ml of the same buffer containing glucose at various concentrations. The absorbance of the dispersion was measured at 436 nm on a Hitachi 330 photospectrometer at room temperature. To avoid any effect of multiple scattering, the linearity between the absorbance and the liposome concentration was checked for the whole absorbance range

observed. The measurements were carried out 1 h after the mixing.

Determination of trapped volume

Liposomes were prepared in the same way except for the presence of [^{14}C]glucose. Extraneous radioactive glucose was removed by passing through a Sephadex G-25 column. The total volume of water trapped in the liposomes was determined from the retained radioactivity on the assumption that there was no change in glucose concentration within the liposomes during the whole process [15]. The molar concentration of phospholipid was determined by phosphorus assay according to the method of Bartlett [16].

Measurements of released [^{14}C]glucose during swelling and shrinking

The condensed dispersion was prepared in the presence of [^{14}C]glucose, and the external radioactivity was removed by passing through a Sephadex G-25 column. 0.3 ml of this stock solution was then pipetted into a test-tube containing 1.2 ml of 475, 100, 37.5, 16.25 or 3.15 mM tracer-free glucose solution in the buffer mentioned above. 1.0 ml was taken from each tube and was dialysed against 10.0 ml of 400, 100, 50, 33.3 or 25 mM (the same concentrations as those in the test-tubes) isotope-free glucose for 4 h by shaking the test-tubes. The radioactivity released was determined by measuring the radioactivity in the external solution.

Results

Scattering efficiency of layered sphere

As can be seen in Eqn. 2, the major factor in turbidity is the scattering efficiency, K_t. To investigate the scattering properties of a multilamellar liposome, scattering efficiency was calculated for a model system according to Eqns 4 and 7. A multishelled sphere composed of alternate lipid and water shells was used as a model of a multilamellar liposome. The geometry of the model is shown in Fig. 1. Refractive indices of lipid (n_l) and water (n_w) were assumed to be 1.497 and 1.340, respectively, and were determined at 20°C for egg-yolk phosphatidylcholine bilayers by using light at 436 nm [17].

The influence of the inner structure of a sphere

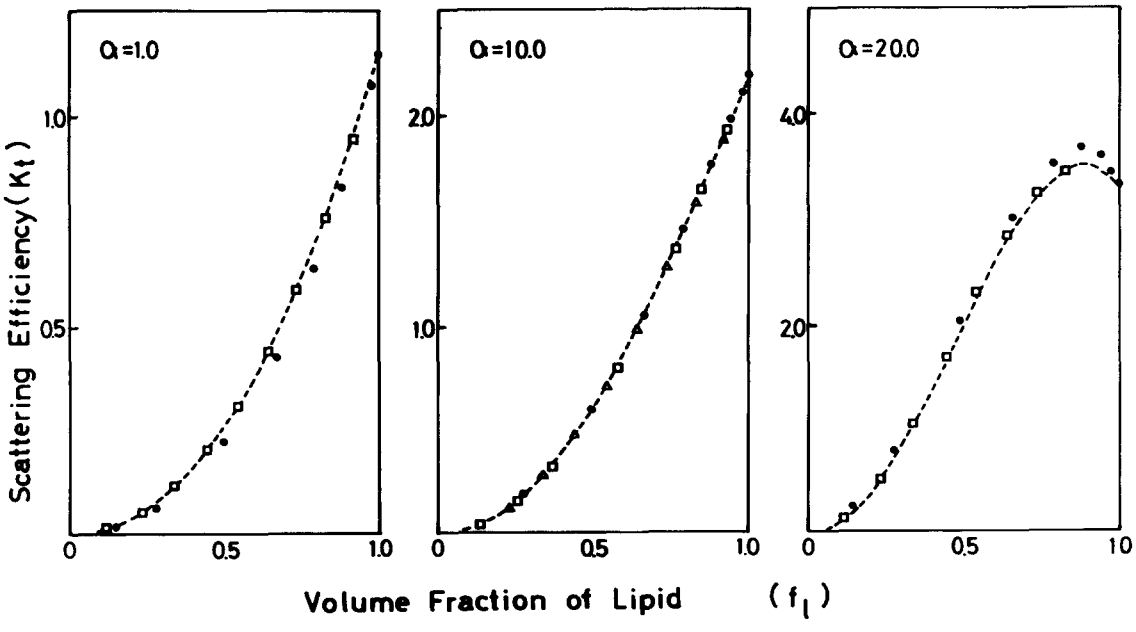

Fig. 2. Relationship between scattering efficiency and the volume fraction of lipid layers for various radius parameters. ●, single-shelled sphere; △, five-shelled sphere; □, ten-shelled sphere; - - - - - -, homogeneous sphere with average refractive index.

on K_t was examined by calculating K_t for the sphere with the same radius but with different lipid shell numbers (1, 5 and 10) at a given lipid fraction. The K_t value obtained is plotted in Fig. 2 as a function of volume fraction of the lipid in the particle (f_l). The relationship between K_t and f_l is insensitive to the number of the lipid layers, irrespective of parameter radius within $1 \leqslant \alpha \leqslant 20$. It follows that the scattering efficiency is determined mainly by the volume ratio of two scattering media (lipid and water) and is scarcely affected by the inner structure of a multishelled sphere. The property of K_t to be insensitive to the inner structure suggests that the contribution of the interfaces of the inner layers is not important. Therefore, K_t of a homogeneous sphere with average refractive index of two components was examined. The average refractive index was calculated according to the following equation, showing the sum rule of polarizability [26]:

$$\frac{n_{av}^2-1}{n_{av}^2+2} = f_l \frac{n_l^2-1}{n_l^2+2} + (1-f_l)\frac{n_w^2-1}{n_w^2+2} \tag{13}$$

where n_{av} is the average refractive index; n_l the refractive index of lipid; n_w the refractive index of water; f_l the volume fraction of lipid in the particle. We can use a simple average of refractive index

$$n_{av} = f_l \cdot n_l + (1-f_l)\cdot n_w \tag{14}$$

if we can assume $n_l/n_w \approx 1$.

The broken lines in Fig. 2 represent the relationship between the K_t value and the volume fraction of lipid. In the case of $\alpha = 10.0$, the K_t values calculated for single-shelled, multishelled and homogeneous spheres fall on the same curve. In the cases of $\alpha = 1.0$ and 20.0, they almost coincide for most f_l values. Especially, K_t values of the ten-shelled spheres are in good agreement with those of homogeneous spheres. It is reasonable that K_t of the sphere with larger number shells shows a better agreement with that of the homogeneous one, since an infinitely numbered shell sphere would be the same as the homogeneous one. The reason of the good agreement must be attributed to the fact that the K_t value of the homogeneous sphere exceeds a little those of the multishelled one at $\alpha = 20.0$ with a cross-over at about $\alpha = 10.0$. Even for a single-shell model, a good agreement with the homogeneous model is achieved at about $\alpha = 10.0$. Consequently, it can be said that

$$K_t(\alpha, n_l, n_w, \text{number and thickness of layers}) \equiv K_t(\alpha, n_{av}) \tag{14}$$

for multishelled spheres with $1 \leqslant \alpha \leqslant 20.0$, $n_w = 1.340$ and $n_l = 1.497$. The parameter radii, 1.0 and 20.0 at 436 nm correspond to a diameter of 1036 and 20720 Å, respectively.

In summary, the turbidity of a liposome suspension can be calculated on the knowledge of the liposome radius and lipid fraction using a homogeneous sphere model. The effect of the osmotically induced swelling or shrinking on the turbidity was investigated employing this method.

Osmotically induced turbidity change

The osmotically induced uptake or release of water affects not only the radius of the particle but also the volume fraction of lipid. Both of them affect turbidity of the liposome suspension. At a constant concentration of liposome, turbidity is proportional to $\alpha^2 K_t$ as shown in Eqn. 2. $\alpha^2 K_t$ was evaluated for a homogeneous sphere with different water volume. Calculated $\log(\alpha^2 K_t)$ is plotted as a function of $\log(\alpha/\alpha_{ini})$ in Fig. 3, where α_{ini} is the parameter radius of the particle without water. Calculation was carried out for $\alpha_{ini} = 1.0$, 2.0, 3.0, 4.0, 5.0, 10.0 and 20.0. The radius was changed from α_{ini} to $3.0 \times \alpha_{ini}$ in each case. Namely, the water content of the particle covers the range from zero to 96.3%. The plots can be fitted to a linear plot for $2 \leqslant \alpha_{ini} \leqslant 5$. The slope which gives the power dependence of turbidity on radius, is also similar for those plots. It shows that turbidity is reciprocally proportional to α^2 or the two-thirds-power of the volume of a particle, not exactly, but practically. At high water content, however, the same relationship holds true for a wider range. The plots deviate from linearity in the vicinity of α and f_l which give the maximum scattering efficiency, as can be seen in Fig. 2. The maximum is achieved under $\alpha = 2/(m_{av} - 1)$ where $m_{av} = n_{av}/n_w$ [18]. Judging from Fig. 3, a simple rela-

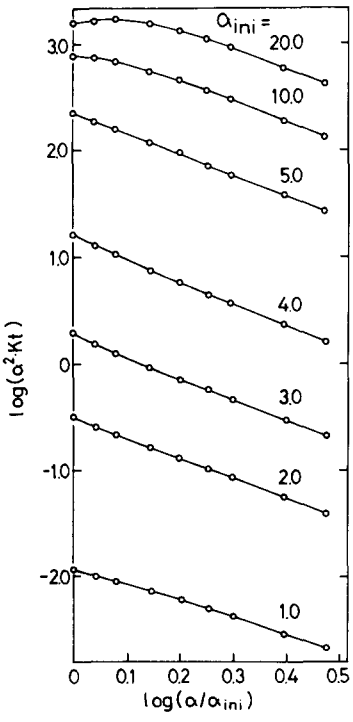

Fig. 3. Calculated value of $\log(\alpha^2 K_t)$ of sphere as a function of $\log(\alpha/\alpha_{ini})$, changing water content. The slope of a plot gives the power dependence of turbidity on radius. The initial parameter radius of the sphere, which corresponds to 'no-water' case, is presented to the right of each plot.

tionship

$$1/\tau \propto V^{2/3} \text{ or } V \propto (1/\tau)^{3/2} \tag{15}$$

is maintained in the range of

$$2 \leqslant \alpha \leqslant \frac{1}{2(m_{av}-1)} \tag{16}$$

As is well known, an actual liposome preparation shows a wide distribution in size. The effect of the size distribution was examined assuming a log-normal distribution of the particle size (see Theory). Fig. 4 shows the relationship between relative turbidity and swelling factor. The initial value of the average particle size, where the particle contains no water, was postulated as 1.0, 5.0 and 10.0 with various standard deviations (1.0, 1.5 and 3.0). The size distributions used are illustrated in Fig. 5. The size distribution of liposomes determined by negative-stain electron microscopy shows similar features [25].

The plots in Fig. 4 show that the volume is still reciprocally proportional to the 3/2 power of the turbidity for all distributions examined. The wider is the distribution, the smaller is the change of turbidity.

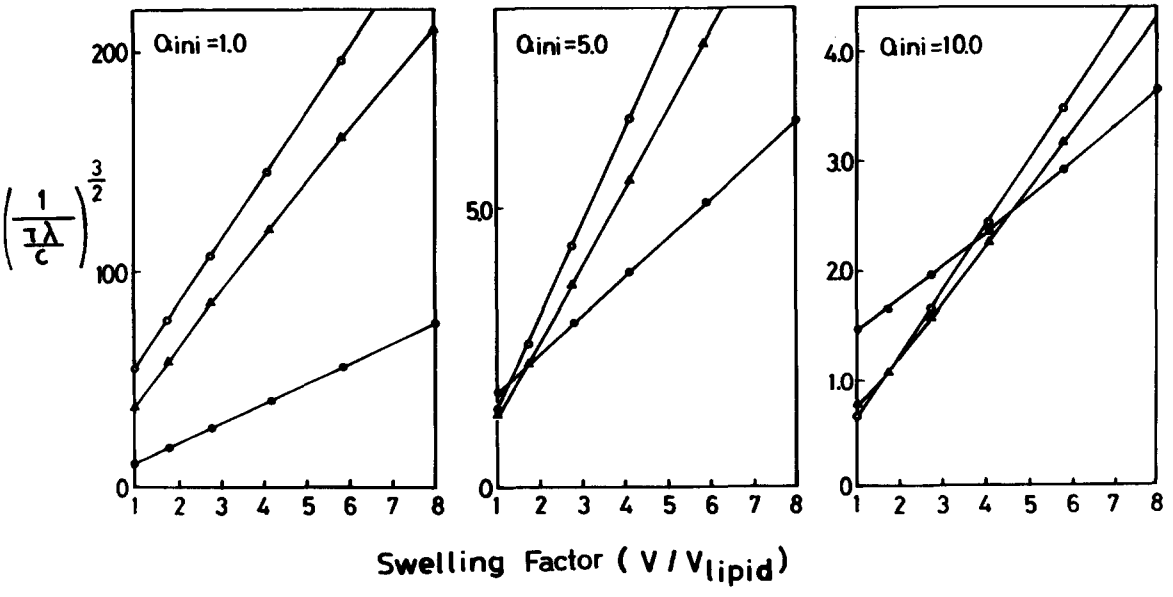

Fig. 4. The relationship between relative turbidity ($\tau/c\lambda$) and swelling factor. ○, homogeneous size; △, standard deviation in size distribution is 1.5; ●, standard deviation in size distribution is 3.0.

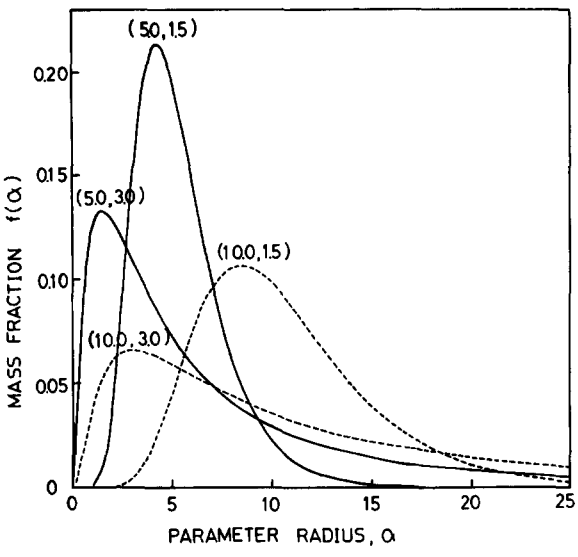

Fig. 5. Typical log-normal size distribution curves. Each pair of numbers denotes the geometric mean radius (α_{50}) and the standard deviation (σ) in the fashion of (α_{50}, σ).

Therefore, it can be said that the particle size distribution affects the extent of the turbidity change but not the power-dependence of turbidity on the volume.

Osmotic behavior of egg-yolk phosphatidylcholine and phosphatidic acid

The trapped water fraction of multilamellar liposomes of egg-yolk phosphatidylcholine and phosphatidic acid (96 : 4) was determined using radioactive glucose. The elution pattern of the liposomes carrying [^{14}C]glucose from a Sephadex G-25 column is illustrated in Fig. 6.

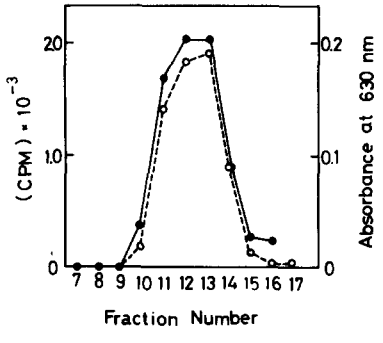

Fig. 6. Elution pattern of multilamellar liposomes of egg-yolk phosphatidylcholine and phosphatidic acids (96 : 4) from a Sephadex G-25 column. ○, absorbance at 630 nm in the phosphorus assay; ●, counts of [^{14}C]glucose. Multilamellar liposomes were prepared in the presence of 100 mM glucose containing [^{14}C]-glucose.

Since the peak of phospholipid coincides with that of radioactivity, the liposomes evidently contain glucose. The phospholipid concentration of each fraction was determined by phosphorus assay. The trapped water volume was 1.8 l/mol phospholipid. The volume fraction of water in the liposomes can be estimated to be 0.69, using the average molecular weight, 780, and the density of the lipid bilayer, 1.056 [19] for egg-yolk phosphatidylcholine. Assuming that the refractive indices of lipid bilayer and water are 1.497 and 1.340, respectively, the average relative refractive index, $m_{av}(=n_{av}/n_w)$ can be also estimated as 1.033 according to Eqn. 13. This value is quite close to that reported for bacteria, 1.044 [7].

For this multilamellar liposome suspension, the osmotically induced turbidity change was examined. When multilamellar liposomes act as perfect osmometers, the total volume of liposomes, V_{total}, changes according to the following equation [1,2]:

$$V_{total} = k/C_{out} + V_{dead} \quad (17)$$

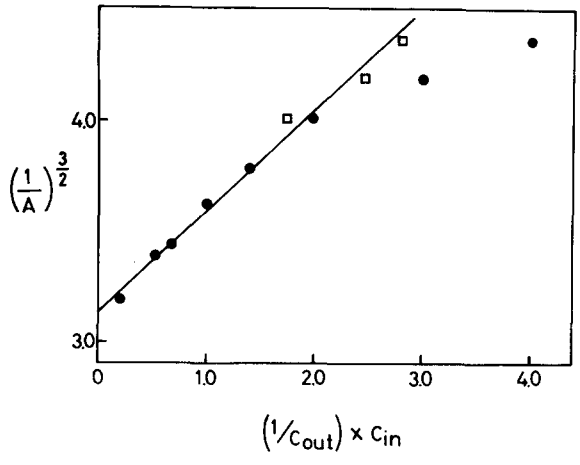

Fig. 7. The reciprocal 3/2 s power of absorbance at 436 nm of liposomes of egg-yolk phosphatidylcholine and phosphatidic acids (96 : 4) as a function of the osmotic gradient across the membrane (●). 0.2 ml of dispersion, prepared in the presence of 100 mM glucose, was diluted with 3.0 ml of glucose solution at appropriate concentration. □, corrected for the leakage of the glucose (see text).

TABLE I

RELEASE OF GLUCOSE FROM LIPOSOME UNDER VARIOUS CONDITIONS

C_{in}/C_{out}:	Hyper-tonic 0.25	Iso-tonic 1.0	Hypotonic 2.0	3.0	4.0
Released glucose (%)	7.0	4.0	17.0	18.0	30.0

where C_{out} is the glucose concentration of the external solution, V_{dead} is the osmotically inactive volume of the liposomes and k is a constant. Since V_{total} is proportional to $(1/\tau)^{3/2}$, $(1/A)^{3/2}$ is plotted as a function of $1/C_{out}$ in Fig. 7. Here, absorbance (A) is equal to ($\tau/2.303$). A linear relationship can be seen under hypertonic ($C_{in}/C_{out} < 1.0$) and hypotonic conditions up to $C_{in}/C_{out} = 2.0$, as expected from the model calculations. The plots gradually deviate from the linear relationship under more hypotonic conditions. In order to clarify the reason of the change of the slope, the release of [^{14}C]glucose from the liposomes during the swelling and shrinking was examined. The results are shown in Table I.

The percentage of released glucose under hypotonic conditions is much higher than that under iso- and hypertonic conditions. Then, the actual osmotic gradient would be smaller due to the release of the trapped glucose. The effective C_{in}, C_{in}^{eff}, can be estimated by $C_{in}[1.0 - (\text{released percent} - 4.0)/100]$. The value of $(1/A)^{3/2}$ is plotted against (C_{in}^{eff}/C_{out}) in Fig. 7. These plots roughly satisfy the linear relationship. Therefore, this fact supports the idea that the liposomes become leaky under the osmotic pressure over a certain threshold.

Discussion

Some calculations have been performed on light-scattering properties of bacterial cells and lipid vesicles [7,17,20,21]. Although there is a rigorous solution for a sphere given by Mie, none of the calculations has employed it because of complexity in numerical calculations. Under the condition of

$$1 \ll \alpha \ll \frac{1}{m_{av} - 1} \tag{18}$$

K_t is written with Jobst approximation [8] as

$$K_t = 2\alpha^2 (m_{av} - 1)^2 \tag{19}$$

The approximation leads to a following equation for τ [12]

$$\tau = \frac{9}{2}\pi \left(\frac{(dn_{av}/dc)}{n_w} \right)^2 \frac{q^2 \nu}{R^2 \lambda'^2} \tag{20}$$

where q is anhydrous mass of lipid in a vesicle and $\lambda' = \lambda/n_w$. It does give the $(1/R^2)$ dependence of τ, as shown in Eqn. 15. This is natural, since the Jobst approximation is valid at a high water content, which gives small $(m_{av} - 1)$. The turbidity is expressed by the Rayleigh-Gans treatment [22–24] as follows:

$$\tau = \tau_R \times \tfrac{3}{8} \int_0^{\pi} P(\theta)(1 + \cos^2\theta) \sin\theta \, d\theta \tag{21}$$

$$\tau_R = \frac{32}{27}\pi^3 \left(\frac{(dn_{av}/dc)}{n_w} \right)^2 \frac{q^2 \nu}{\lambda'^4} \tag{22}$$

where $P(\theta)$ is the so-called scattering factor, a correction to normal Rayleigh scattering (τ_R) due to the interference of light scattered from different parts of the particles. The function $P(\theta)$ depends on the shape of the particle. Though it is assumed that $2\alpha(m_{av} - 1) \gg 1$ in this derivation, the size and m_{av} of multilamellar liposomes do not meet this assumption. It was suggested, however, that as far as turbidity is concerned, the Rayleigh-Gans method would give precise results even for $2\alpha(m_{av} - 1) \geqslant 1$ [12]. But no simple relationship between τ and R is seen any more.

Our calculation does not involve any assumption as to the size and refractive index of the particle, although a shape change was not taken into account. Our results show that turbidity is reciprocally proportional to the two-thirds power of the volume of multilamellar liposomes at a given concentration. It holds true even under a wide distribution in liposomal size. Such distribution just decreases the extent of the turbidity

change against volume. The range over which this relationship is valid is given by the condition of Eqn. 16. The upper limit is determined by the appearance of the maximum of K_t. The lower limit is associated with the fact that the diameter of the particle is becoming smaller in comparison with the wavelength, which eventually leads to Rayleigh scattering. As can be seen in Eqn. 22, turbidity caused by Rayleigh scattering does not change any further upon swelling or shrinking of the particle. Therefore, the turbidimetric method is not useful for small vesicles, for example, sonicated vesicles. Since α is wavelength-dependent, the method can cover liposomes of 1700–30000 Å diameter (m_{av} = 1.033) by a change in the wavelength of the light from 350 to 800 nm. If the water content is larger than that in the liposomes used in this work, it can cover a wider range of liposomal size. Taking the influence of size distribution of liposomes into account, the method can be used for practically any multilamellar liposomes. The extent of the size distribution can be checked qualitatively by measuring the wavelength dependence of turbidity. The wavelength dependence can be approximated to λ^{-x} in the region 350 to 900 nm. In general, the wider the size distribution becomes, the smaller is the value of x. Theoretically, the infinitely large standard deviation of the size distribution predicts 1 as the value of x, provided that the refractive index does not depend on the wavelength [13]. For example, the multilamellar liposome sample used in this work gives $x = 0.8$, whereas in the case of an *Escherichia coli* cell suspension, x rises to 2.3. The size distribution of the latter should be much narrower. Actually, x becomes 1.5–1.8 when the multilamellar liposomes dispersion is treated with a membrane filter or a Sepharose 4B column.

Another factor which could affect the turbidity of liposomes is the shape of the liposomes. A sphere was assumed in the calculation. It is impossible to compute turbidity of liposomes in a shape other than sphere by using the Mie theory. Koch calculated the turbidity for some ellipsoids with a given volume on the basis of the Rayleigh-Gans approximation. His result showed that their turbidities are smaller than that of a sphere. A change from a sphere to a deformed shape could take place during shrinking. Shrinking induces an increase of turbidity, but it cannot be explained by a change in liposomal shape, since the change of shape from a sphere at a given volume would rather induce a decrease in turbidity. The contribution of a change in shape to turbidity would be small, even if it exists.

The empirical rule proposed by Bangham was that the turbidity is reciprocally proportional to the volume of liposomes. As far as the osmotically induced turbidity change of liposomes is concerned, the extent of the change is so small that the plots can apparently accommodate $\tau \propto 1/v$. For small change in turbidity, Bangham's rule can be used in practice to follow an osmotic change. Although the relationship deduced by him is not correct, his idea of using the turbidimetric method for the investigation of osmotically active liposomes is supported by our results.

As can be seen in Fig. 7, the plots deviate from the linear relationship under extreme conditions. The physical meaning of this phenomenon was clarified by the radioisotope experiments; namely, the lipid bilayer is no longer a barrier to the solute under these conditions. The barrier function is one of the essential properties of a biomembrane. Therefore, the inflexion point corresponds to the limiting condition for the lipid bilayer to be able to function as a barrier in a biomembrane.

Acknowledgements

This work was partly supported by a grant from the Ministry of Education of Japan (No. 510407). All computations were carried out on an ACOS 900 computer at the Crystallographic Research Center, Institute for Protein Research, Osaka University.

References

1 Bangham, A.D., Gier, J.D. and Greville, G.D. (1967) Chem. Phys. Lipids 1, 225–246
2 Rendi, R. (1967) Biochim. Biophys. Acta 135, 333–346
3 Gier, J.D., Manderslooty, J.G. and Van Deenen, L.L.M. (1968) Biochim. Biophys. Acta 150, 666–675
4 Hill, M.W. and Cohen, B.E. (1972) Biochim. Biophys. Acta 296, 403–407
5 Reeves, J.P. and Dowben, R.M. (1970) J. Membrane Biol. 3, 123–141
6 Bittman, R., Leventhal, A.M., Karp, S., Blue, L., Tremblay, P.A. and Kates, M. (1981) Chem. Phys. Lipids 28, 323–335

7 Koch, A.L. (1961) Biochim. Biophys. Acta 51, 429–441
8 Jobst, G. (1925) Ann. Physik 78, 157–166
9 Bangham, A.D. and Horne, R.W. (1964) J. Mol. Biol. 8, 660–668
10 Chapman, D., Fluck, D.J., Penkett, S.A. and Shipley, G.G. (1968) Biochim. Biophys. Acta 163, 255–261
11 Mie, G. (1908) Ann. Physik 25, 377–445
12 Kerker, M. (1969) The Scattering of Light and Other Magnetic Radiation, Academic Press, New York
13 Yang, K.C. and Hogg, R. (1979) Anal. Chem. 51, 758–763
14 Comfurius, P. and Zwaal, B.F.A. (1977) Biochim. Biophys. Acta 488, 36–42
15 Roseman, M.A., Lentz, B.R., Sears, B., Gibbes, D. and Thompson, T.E. (1978) Chem. Phys. Lipids 21, 205–222
16 Bartlett, G.R. (1959) J. Biol. Chem. 234, 466–468
17 Chong, C.S. and Colbow, K. (1976) Biochim. Biophys. Acta 436, 260–282
18 Born, M. and Wolf, E. (1975) 'Principles of Optics', Pergamon Press, Oxford
19 Rahrja, R.K., Kaur, C., Singh, A. and Bhatia, I.S. (1973) J. Lipids Res. 14, 695–697
20 Senfert, W.D. (1970) Biophysik 7, 60–73
21 Tinker, D.O. (1972) Chem. Phys. Lipids 8, 230–257
22 Rayleigh, Lord (1881) Phil. Mag. 12, 81–101
23 Rayleigh, Lord (1914) Proc. R. Soc. Lond. Ser A 90, 219–225
24 Gans, R. (1925) Ann. Physik 76, 29–38
25 Olson, F., Hun, C.A., Szoka, F.C. and Papahadjopoulos, D. (1979) Biochim. Biophys. Acta 557, 9–23
26 Yi, P.N. and MacDonald, R.C. (1973) Chem. Phys. Lipids 11, 114–134